



Article

Economic Analysis of a Redox Flow Batteries-Based Energy Storage System for Energy Savings in Factory Energy Management System

Seon Hyeog Kim * , Yoonmee Doh, Tae-Wook Heo and Il Woo Lee

Environment ICT Research Section, Industry & Energy Convergence Research Division, Electronics and Telecommunications Research Institute (ETRI), Daejeon 34129, Republic of Korea; ydoh@etri.re.kr (Y.D.); htw398@etri.re.kr (T.-W.H.); ilwoo@etri.re.kr (I.W.L.)

* Correspondence: seonh@etri.re.kr

Abstract: Renewable energy systems are essential for carbon neutrality and energy savings in industrial facilities. Factories use a lot of electrical and thermal energy to manufacture products, but only a small percentage is recycled. Utilizing energy storage systems in industrial facilities is being applied as a way to cut energy costs and reduce carbon emissions. However, lithium-based batteries, which are predominantly used in traditional industries, face challenges in terms of affordability and reliability. Redox flow batteries, on the other hand, offer high power output and reliability, and are economical to manufacture for installations with high capacity. Although redox flow batteries are difficult to use in general electrical systems due to their small volume-to-capacity ratio, they can be easily utilized as energy storage devices in industrial parks or renewable energy parks with relatively little space constraints. In addition, since factories use a lot of heat energy in addition to electricity, utilizing combined heat and power can further reduce heat energy. In this study, we analyzed the cost estimation and economic feasibility of utilizing photovoltaics, redox flow cells, and combined heat and power to save energy in a factory's energy management system.



Citation: Kim, S.H.; Doh, Y.; Heo, T.-W.; Lee, I.W. Economic Analysis of a Redox Flow Batteries-Based Energy Storage System for Energy Savings in Factory Energy Management System. *Batteries* **2023**, *9*, 418. <https://doi.org/10.3390/batteries9080418>

Academic Editors: Sreenivas Jayanti and Ravendra Gundlapalli

Received: 6 July 2023

Revised: 2 August 2023

Accepted: 7 August 2023

Published: 10 August 2023



Copyright: © 2023 by the authors. Licensee MDPI, Basel, Switzerland. This article is an open access article distributed under the terms and conditions of the Creative Commons Attribution (CC BY) license (<https://creativecommons.org/licenses/by/4.0/>).

1. Introduction

Carbon neutrality aims to achieve emitting zero greenhouse gases into the environment; greenhouse gases are the primary cause of global warming. To achieve carbon neutrality, there is an increasing interest in the active deployment of renewable resources and highly efficient power systems that can efficiently utilize existing energy. To achieve the 2050 carbon neutrality goal, we need to limit the temperature growth to 1.5 degrees Celsius below the global average temperature of about 100 years ago, before industrialization, and this will require an annual reduction of 36.9 Gt of greenhouse gases. Since the main emitters of greenhouse gases are the industries that use the most energy, achieving carbon neutrality requires replacing fossil fuel power generation, which is a major source of greenhouse gases, in the power and energy sectors. To reduce greenhouse gases, fossil fuel power generation must be reduced and replaced with carbon-free power sources utilizing renewable energy. However, renewable energy sources cannot provide a stable power supply due to large fluctuations in output depending on climate conditions, so it is difficult to supply and receive power alone. Without energy storage, a renewable power generation rate of more than 10% will cause instability of the entire grid and severe damage to power quality. Recent studies estimate the limit of grid-connected renewable generation to be 10–15% [1–3].

Recent large-scale blackouts in California (2020) and Texas (2021) are prime examples of renewable energy reliability issues, as these regions have some of the largest solar

and wind deployments in the U.S., respectively, and are highly dependent on renewable energy. Therefore, in order to overcome the intermittency and volatility of these renewable energies and operate stably, it is necessary to deploy and utilize long-term energy storage systems (ESS). There are various technologies for ESS, including flywheels, secondary batteries, energy storage using compressed air, pumped storage, and supercapacitors. Lithium-based secondary batteries, which have been widely used recently, are mainly used for short-term ESS such as electronics and electric vehicles, and are not ideal for long-term ESS in large power systems due to reliability and cost issues. While supercapacitors and flywheels have a long lifespan, they are optimized to provide energy for short periods of time (10 min or less), so they are not ideal for long-duration ESS that need to store or deliver energy for extended periods of time. ESS utilizing pumped storage or compressed air have the disadvantage of being difficult to install due to their large installation scale, space constraints, and very high initial construction costs [4–6].

To manage and reduce high energy consumption in factories, it is necessary to develop and implement a factory energy management system (FEMS). A FEMS installs measurement systems in existing factory facilities and monitors and analyzes them in real time to derive energy saving measures. In addition, control and operation systems can be utilized to engage in optimal process production and energy operation. It can be utilized in conjunction with systems such as renewable energy, energy storage, and CHP to further save energy.

Rechargeable batteries make a significant contribution to solving energy-saving problems in industrial facilities, and recent research continues to enhance the structure and performance of these batteries [7]. Redox flow batteries (RFB) are a kind of secondary battery that, similarly to lithium-ion batteries (LIBs), store electrical energy through redox reactions. The main difference from LIBs is that a typical LIB consists of a solid electrode and a liquid electrolyte, while an RFB consists of a liquid mixture of electrolyte and active material that is circulated by a pump. The atoms used in RFBs, such as vanadium, have a lower energy density than lithium, which has a very high capacity, and RFBs are less energy efficient than LIBs because they require constant pumping to control liquid flow. However, they are cheaper than LIBs, have very good cycle characteristics, and are non-flammable, making them more reliable batteries. Therefore, RFBs require more specific applications than LIBs to be applied to real-world infrastructure, and the idea of applying them to ESS, which requires the highest reliability, is currently being explored [8,9]. One proposed novel framework for multiobjective and multi-criteria optimization (levelized cost of electricity (LCOE)) is stated to simultaneously reduce the charging time and energy loss of a battery in charging mode [10]. Numerical studies are a useful method for evaluating several major parameters that are essential for optimizing an energy system based on redox flow battery technology [11]. The authors of [12] investigated development analytics and economic models for capacity optimization, the minimum operating cost, and determining the optimal mix of PV-ESS in a utility-grid system. Energy consumption is primarily met by the PV-ESS or by purchasing energy from the grid whenever the energy generated by the PV-ESS is not enough to meet the demand. The excess PV energy generated is used for the ESS to charge, and any surplus energy is sent back to the utility grid. Furthermore, with artificial intelligence (AI)-based time series forecasting greatly improving performance predictions and research on remaining capacity of ESS, energy savings from optimal operation are optimistic [13]. AI is being applied to solve structural problems and improve reliability in energy storage devices, and researchers are proposing the use of automated machine learning to learn optimized structures to overcome the enormous complexity of the structural properties of perovskite materials [14,15]. In the case of RFBs, advances in redox-targeted flow battery technology provide a reliable solution for future large-scale electrochemical energy storage. Structural improvements and performance management for these battery materials are expected to increase energy efficiency and reduce deployment costs [16].

Combined heat and power (CHP) is a highly efficient method of generating electricity and heat simultaneously in a single integrated system. In a conventional energy system,

power plants generate electricity, and the extra heat generated during the generation process is usually wasted. In a CHP system, however, this waste heat is captured and utilized for a variety of heating and cooling purposes, such as providing hot water, heating a space, or powering an industrial process. A dispatching model with a CHP unit, a thermal unit, and a variable RES that balances all heat and power production is proposed in [17]. A test and evaluation system is investigated to verify the accuracy and efficiency of the performance of the proposed model. A sensitivity analysis of the LCOE for a system combining renewables, batteries, and CHP is presented in [18]. Based on the analysis of different costs for the three components, this paper examines the economic feasibility in a traditional grid. However, there has been no analysis of utilizing these systems in factories.

This study examines the economics of implementing the three systems in a factory. The applied factories are two factories in the bio and paper industries, and the characteristics of power and heat loads are analyzed based on actual operational data to estimate the savings in both heat and power energy that can be achieved by adopting hybrid energy systems. Since hybrid energy systems are expensive to introduce, we analyze their economic feasibility based on LCOE, assuming a scenario where they are shared by both plants. Thus, the three technological advances of solar, batteries, and CHP have increased the likelihood that a significant number of utility customers will go off-grid (move to a completely independent power grid), a phenomenon that is expected to increase in the future. In this paper, we quantify the economics of deploying a hybrid energy system incorporating solar, batteries, and CHP in a factory by calculating the LCOE. Sensitivity analysis is performed on factors such as installed capacity of the three components, operation and maintenance costs, capital costs, power factor of PV and the capacity of CHP, financing terms, and the cost of natural gas. The results presented allow us to examine the economics and applicability of PV, CHP, and vanadium redox flow batteries (VRFB) in industrial parks.

2. ESS Solutions in Industry

When introducing renewable energy in industrial complexes, solar power generation is mainly introduced due to space constraints, but output limitation is often a problem due to the amount of power generation concentrated in the daytime. In addition, since solar power generation is not sufficient in the early morning and evening hours, turbine generators must be used to resolve peak loads, which generate greenhouse gases. To solve these problems, a large-capacity and long-duration ESS that can discharge to peak loads and continuously discharge for a long time to shift loads to other time zones is needed.

As of 2021, the installed capacity of countries actively promoting grid-scale ESS is shown in Figure 1 (2.9 GW in the U.S., 1.9 GW in China, 1.0 GW in Europe, and 0.1 GW in South Korea). Among them, California, which is actively utilizing solar power generation, is expected to require up to 11 GW of long-term ESS by 2030, assuming that 60% of electricity is supplied by renewables. The International Energy Agency's (IEA) net-zero scenario, which is aggressive in its adoption of long-duration grid-type storage, calls for a significant increase in battery storage capacity, especially at the grid scale. In the IEA's scenario, installed grid-scale battery ESS capacity increases 44-fold between 2021 and 2030 to 680 GW. About 140 GW of capacity will be additional in 2030 alone, up from 6 GW in 2021. Achieving the net-zero scenario requires a significant increase in annual capacity additions, averaging more than 80 GW per year between 2022 and 2030 [19].

ESS can improve energy efficiency, making electricity more affordable and sustainable. The objectives and requirements for utilizing ESS in factories and industrial parks are outlined in the following section.

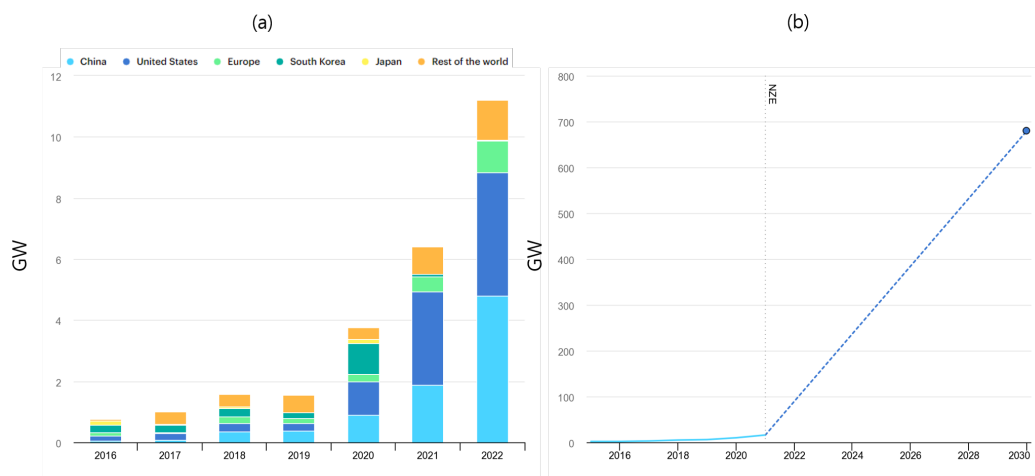


Figure 1. (a) Grid-scale battery ESS capacity added per year, 2016–2022; (b) grid-scale battery ESS installed in the IEA's scenario, 2015–2030. Reprinted from Ref. [19].

2.1. Demand Response

ESS that can be utilized in factories are considered to be highly useful for reducing electricity bills through demand response, reducing peak power, and incentivizing energy sharing by ESS. CHP and ESS can be installed to reduce the energy usage of boilers and chillers used in the factory to achieve load leveling effects. In factories, heat demand by time of day/season has a different pattern from the total power demand of the factory power system, so utilizing ESS for heating and cooling CHP can help reduce peak load. The heat demand of a boiler has a pattern of rising, falling, rising, falling, rising, falling, rising, falling through spring, summer, fall, and winter. Conversely, the chiller's chilled water demand is concentrated in the summer months. Similarly, the boiler's heat demand is highly volatile, with a large spike in the winter months. In addition, since there are differences in demand by time of day depending on the temperature of the atmosphere, it is possible to reduce peak load by storing energy in the early morning hours when demand is minimal and discharging it during peak demand. Therefore, it is a suitable system for saving electricity and thermal energy according to demand response, so operators can expect energy savings by installing an ESS suitable for CHP.

2.2. Peak Reduction

ESS can be used by the electricity grid to meet the high intensity loads that occur during peak hours. ESS alleviate peak loads by providing power to the grid by charging during peak hours and discharging when it is needed. An ESS can be integrated with an energy management system (EMS). An EMS is a system that improves the efficiency of the grid by monitoring and controlling power demand and production in real time. An ESS can be used in conjunction with the power system to optimize electricity demand forecasting and load management.

2.3. Stabilizing Renewable Energy

ESS can be integrated with renewable energy systems to mitigate the instability of electricity supply and demand. Renewable energy relies on natural conditions, such as sunlight and wind, to produce electricity, which can be unpredictable. An ESS improves the reliability of the grid by storing overproduction of renewable energy and delivering renewable energy when needed.

3. Energy Saving Systems in Factories

Factories can reduce their electricity cost by utilizing distributed energy resources (DER) that can be installed on their site or DERs from the surrounding power system. Since the production and output of PV, wind, etc., utilized as DER do not have a constant

output, ESS can be used to store electricity and deliver it to the factory's power system at the moment of need [4].

3.1. FEMS

A FEMS is a scheme for monitoring and managing energy use. The system helps to enhance the energy efficiency of a factory and reduce energy consumption. A FEMS can be divided into configuration levels based on the relevant infrastructure and functions. Based on infrastructure, it consists of measurement infrastructure (sensors, meters, PLC, DCS, etc.) that measure operational data from utility facilities and process facilities, data collection devices (Edge GateWay) that acquire measurement data from the measurement infrastructure, and data acquisition and storage devices (data acquisition systems) that store and manage collected data in the system. Functionally, it consists of an Energy Information System (EIS) that performs energy monitoring, statistics and analysis, and energy performance management, and an Energy Optimization System (EOS) that reduces inefficient parts of energy consumption. Figure 2 shows the conceptual components and functions of a FEMS.

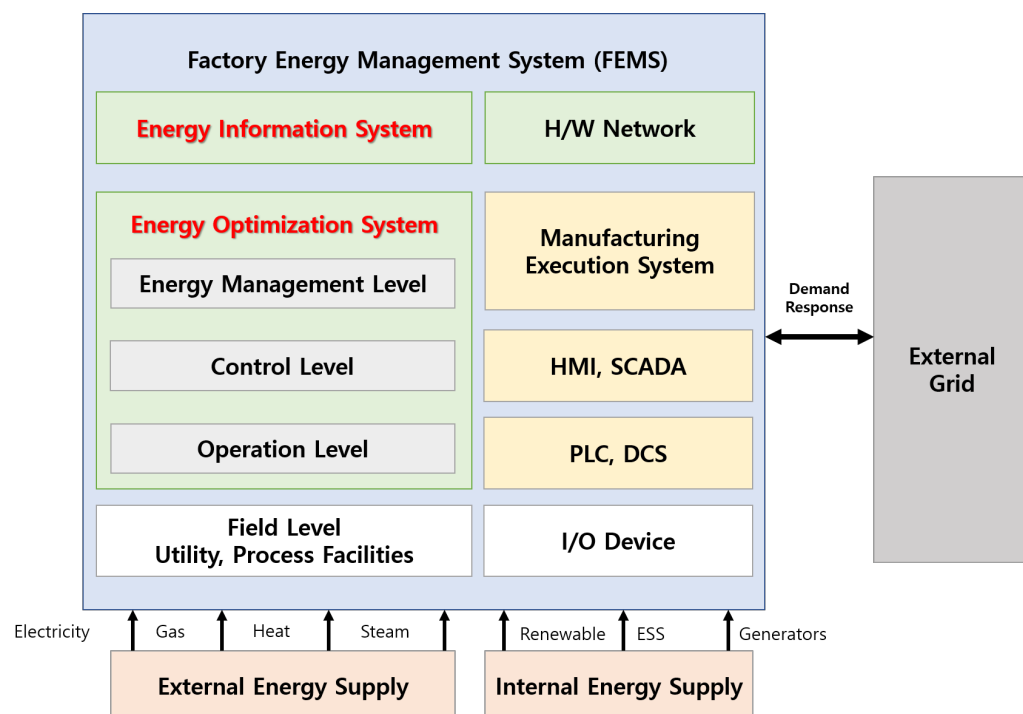


Figure 2. Factory energy management system components and functions.

3.1.1. EIS

EIS uses the collected data to provide services such as energy monitoring, statistics and analysis, and energy performance management. Through EIS, factory operators can evaluate energy consumption and potential savings through facility monitoring, set goals, identify improvements, and take actual savings measures. EIS operates based on the energy saving process evaluated by the ISO 50001 energy management system.

3.1.2. EOS

EOS can include energy optimization for utility facilities such as air compressors, boilers, chillers, etc., or energy optimization for production processes by analyzing the energy consumption factors of production process facilities and optimizing them. Examples of the latter include excessive energy input to prevent product defects, energy operation with fixed settings regardless of load fluctuations, waiting time, leakage energy, and manual operation, which causes fluctuations in production quality and energy operation depending

on the proficiency of field operators. In the past, energy optimization was mainly centered on replacing high-efficiency equipment, but recently, the paradigm of energy efficiency has changed to energy optimization centered on intelligent information based on renewable energy and AI. EOS is divided into levels for each purpose: the field level, which consists of utility and process facilities; the control/operation level, which performs monitoring-based control by measuring and collecting data on facility operations; and the energy management level, which manages energy performance.

4. Redox Flow Battery

To build ESS in factories and industrial complexes, secondary batteries with high capacity and long cycle life are required. Among RFBs, VRFBs have recently been applied to the demonstration of industrial complexes. There are different kinds of flow batteries, depending on the active substance and chemical reaction principle, but based on the global commercialization performance and distribution of related companies, the vanadium-based VRFB is the most representative and currently available technology. VRFBs are attracting attention as the next generation of industrial ESS due to their low cost, stability, long life, and ease of disposal compared to lithium-based secondary batteries.

4.1. Fire Safety

VRFBs use a vanadium ion electrolyte, which is soluble in water rather than organic solvents, and this aqueous solution flows throughout the redox flow cell at a low temperature of 20 to 40 degrees Celsius, eliminating the fire hazard that is often associated with LIBs. Compared to LIBs, the most common secondary battery (VRFBs) are characterized by the separation of the electrical energy storage. VRFBs store energy in the electrolyte, which is in a liquid state, compared to the positive and negative electrodes of a typical secondary battery. Therefore, there is no need for a separator (e.g., a secondary battery), so there is no possibility of fire due to damage to the separator, which is the main cause of fire in lithium-ion batteries, and it is safe from fire because the energy is stored in the electrolyte, not the cathode and anode. This reliability is an advantage for industrial parks and power generators which are sensitive to the safety of ESS fires.

4.2. Long Cycle Life

Compared to RFBs that use other electrolytes for oxidation/reduction, such as Zn/BR, Fe/CR, etc., VRFBs use the same vanadium ion for both anode and cathode, so even if they pass from one pole to another through a separator, they react to the characteristics of each pole with oxidation and reduction reactions again, resulting in a longer lifespan than other RFBs. VRFBs have the longest lifespan of any commercially available battery at 20 years and over 20,000 cycles. VRFBs have a relatively long life compared to other batteries for two reasons: (1) charging and discharging by surface reaction and (2) electrolyte re-balancing. In conventional batteries, the active material is charged and discharged by the surface or internal plating of the electrodes (bulk reaction), but this reaction is not 100% reversible, so the usable energy capacity decreases with increasing charge and discharge cycles. On the other hand, in the case of VRFB, only the ionic state of vanadium dissolved in the electrolyte changes, and the electrode is utilized only as a conduit for electrons (surface reaction), so the available energy decreases very little with increasing charge/discharge cycles. The re-balancing of VRFBs is unique to all-vanadium flow batteries, where the anode and cathode have exactly the same material and structure, so there is no crossover of unwanted ions or water between the separators, even over long periods of operation. If crossover occurs, the balance of ions in the anode and cathode is disrupted, resulting in a decrease in energy capacity.

4.3. Ease of Maintenance

Compared to Li-ion batteries, there is a major difference in electrolyte utilization. While the electrolyte in a lithium-ion battery is utilized as a medium to pass lithium ions

between the anode and cathode, VRFBs play an important role in storing electrical energy in the electrolyte itself. The electrolyte of a VRFB contains vanadium, an activating material, and is charged and discharged by the redox reactions of vanadium-ions. In addition, since the electrodes and electrolyte that make up the anode and cathode are made of the same material, VRFBs are also advantageous in terms of maintenance, as the internal chemical composition of the battery does not change even during long-term operation, reducing the possibility of chemical side effects. Because it uses the same electrolyte, the structure of the ESS is simpler than other battery-based energy storage devices, and because there are no byproducts such as hydrogen generated by some RFBs, there is no need for a separate processing unit, making it easier to operate.

4.4. Easy to Increase Energy Capacity

VRFBs are also different from general energy storage devices in terms of capacity and output. In a typical battery, both power and energy are determined by the electrodes, but in a VRFB, energy is determined by the amount of electrolyte and output is determined by the stack containing the electrodes. Due to these features, VRFBs can be designed with independent power and energy capacities, and are especially suitable for large-capacity and long-cycle ESS implementations because the ratio of energy to power can be relatively high. Since the capacity of the VRFB is determined by the volume of the electrolyte tank, expanding their capacity in the future is also easy: simply increasing the volume of the electrolyte can easily increase the capacity of the VRFB.

4.5. Easy to Recycling

In addition to carbon neutrality, recyclability is an important factor for energy resources these days, and VRFB is highly recyclable. The vanadium electrolyte used has a similar residual value at the end of the 20-year operational life as it did at the beginning, so the vanadium can be extracted and recycled even after the end of operation.

5. CHP Systems

In addition to VRFB, industries are interested in energy savings and lower operating costs by utilizing CHP. CHP is a power generation method that simultaneously generates electricity and provides heat to improve overall energy utilization. Because it can generate and supply both electricity and heat, it is highly energy efficient and has a significant greenhouse gas reduction effect to achieve net-zero. CHP technology utilizes heat wasted in the production of electricity to provide both electrical power and useful thermal energy from a single source. CHP is efficient and cheaper than providing heat and electricity energy separately, which generally requires the use of more fuel. The concept of a CCHP system refers to the process of using heat produced by CHP to power an absorption chiller or direct-fired chiller to generate chilled water for applications such as air conditioning or refrigeration in addition to electricity and heat production. As shown in Figure 3, the U.S. Energy Information Administration's (EIA) Annual Energy Outlook forecasts future demand for CHP in industrial applications. Figure 3 shows that capacity and generation for CHP will continue to grow over the next 30 years, reaching 36 GW of capacity and 200 BkWH of generation in 2050 to achieve eventual carbon neutrality [20].

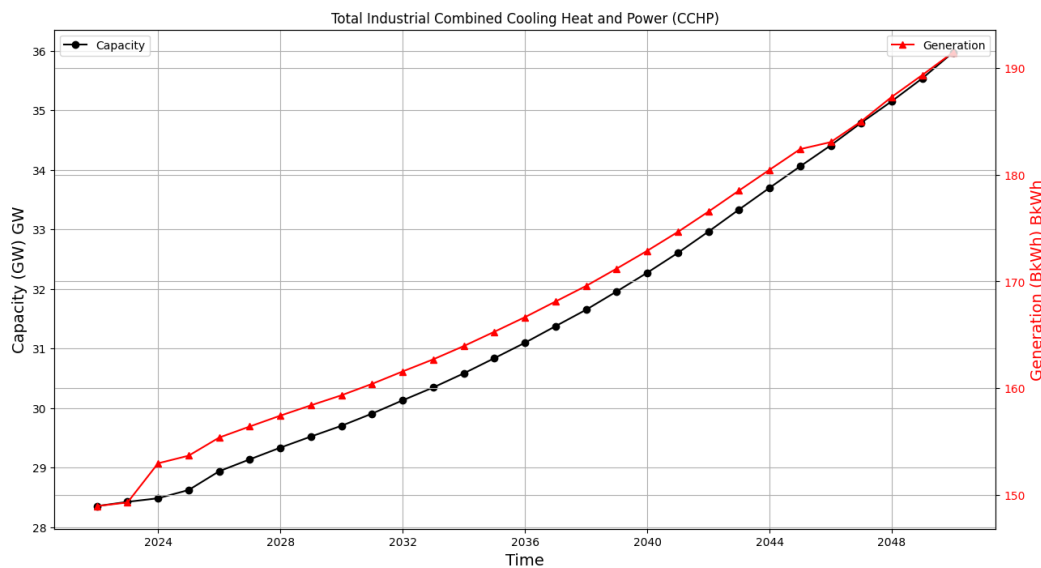


Figure 3. Total industrial combined cooling heat and power. Reprinted from Ref. [20].

6. System Modeling

Calculating the overall cost and payback of installing PV, CHP, and ESS in a factory to reduce carbon and thermal/electrical energy is a complex process and is affected by many variables. Specifically, the detailed specifications of each technology, installation and operating conditions, electricity tariff structures, and investment costs must be considered. LCOE is calculated by applying modeling based on actual operational data. This requires information such as the factory's operational profile, power demand patterns, existing infrastructure configuration, etc. In this study, simulations are performed based on the operational data of a factory that intends to deploy FEMS and energy saving devices for actual energy savings.

VRFB and CHP can be applied to factories to reduce thermal and electricity energy costs, but the initial cost of infrastructure construction is very high, and it may take a long time to recover the investment cost. To overcome these limitations, an ESS deployment environment that can be shared by multiple factories can be proposed. Figure 4 shows a plan for Factory A and Factory B to share an ESS to save energy. A suitable renewable energy source for the factory is PV, which can be deployed on the roof and on the factory grounds. Both Factory A and Factory B contain equipment with high electrical energy consumption for manufacturing, such as conveyor belts, compressors, pumps, and motors. In addition, the lighting system for workers in the factory is a power load that remains constant regardless of the manufacturing process. If a heating process is required, the process may include boilers, furnaces, and heat pumps, which are among the highest of the major loads. Similarly, if a cooling and chilled water system is required, refrigeration devices such as chillers and cooling towers are deployed and must be operated according to the outside temperature and the temperature/humidity inside the factory, making it a highly variable load. In addition, welding machines, air compressors, freezers, and dehydrators are other examples of high load equipment in the factory. As shown in Figure 4, in Factory A, the cooling and chilled water systems account for a high proportion of the energy used for manufacturing, while in Factory B, the heating system is the main load. Both electricity and thermal energy consumption can be reduced by operating complementary systems with different patterns of thermal energy consumption.

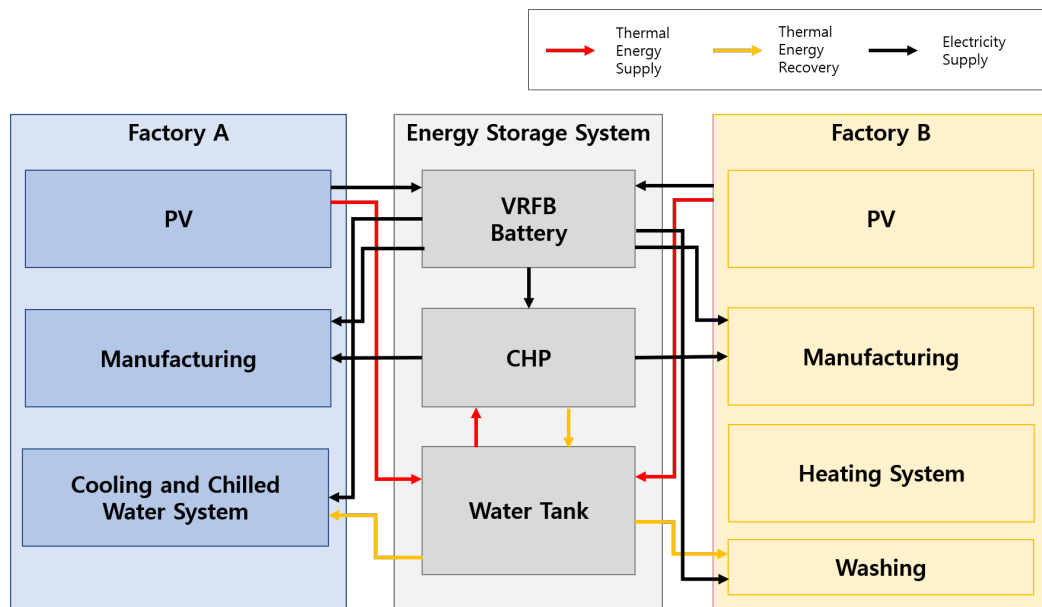


Figure 4. ESS sharing structure between factories.

6.1. Time-of-Use and Seasonal Electric and Thermal Energy Tariff

Time-of-use power and heat pricing is a system where user's rates vary based on user's power and heat usage during different times of the day. As shown in Figure 5, a user pays a higher power rate when user power usage is high during peak hours, and a relatively lower power rate during off-peak hours. These time-of-use pricing plans were introduced to maintain grid stability and increase energy efficiency by decentralizing electricity demand. Similarly, time-of-use heat plans have a different pricing structure that varies by season, with higher heat rates during peak heating and cooling hours.

Typically, hourly electricity plans are divided by time of day and into two seasons: summer (June through September) and winter (December through February) and the rest of the year. The demand side's load has different peak and off-peak hours for each season and day of the week, and is charged in tiers categorized by power usage. There are usually three tiers, and the higher the tier, the more expensive the peak hour rate. To take advantage of hourly power plans, it is important to manage the users' power usage efficiently and minimize power consumption during peak hours. The users can do this by utilizing energy storage to shift loads to reduce peak loads, and by charging and utilizing it during off-peak hours.

6.2. Modeling PV

In order to propose the optimal configuration of ESS applied to a factory energy management system, it is necessary to consider process-specific and hourly load patterns, equipment-specific loads, and model the output of the power generation sources supplying the factory and the ESS. The output of solar power is affected by the footprint of the PV module, the insolation of the area where it is installed, and the temperature of the cell, and is given by the following equation:

$$P_{pv} = \eta_{pv} A_{pv} R_t N_{pv} [1 - \lambda(T_c - 25)] \quad (1)$$

where η_{pv} represents the PV module efficiency, A_{pv} represents the footprint of PV modules, R_{pv} represents the insolation per hour, λ is the optimal efficiency operating factor and T_c represents the surface temperature of the PV. Equation (1) models the surface temperature-based output of a PV, where the surface temperature T_c of the PV module is defined as:

$$T_c = T_n + S_{pv}(T_o - 20/k) \quad (2)$$

where T_n represents ambient temperature of PV, T_o represents PV module temperature specified by the system operator, and S_{pv} represents solar insolation per area [21,22].

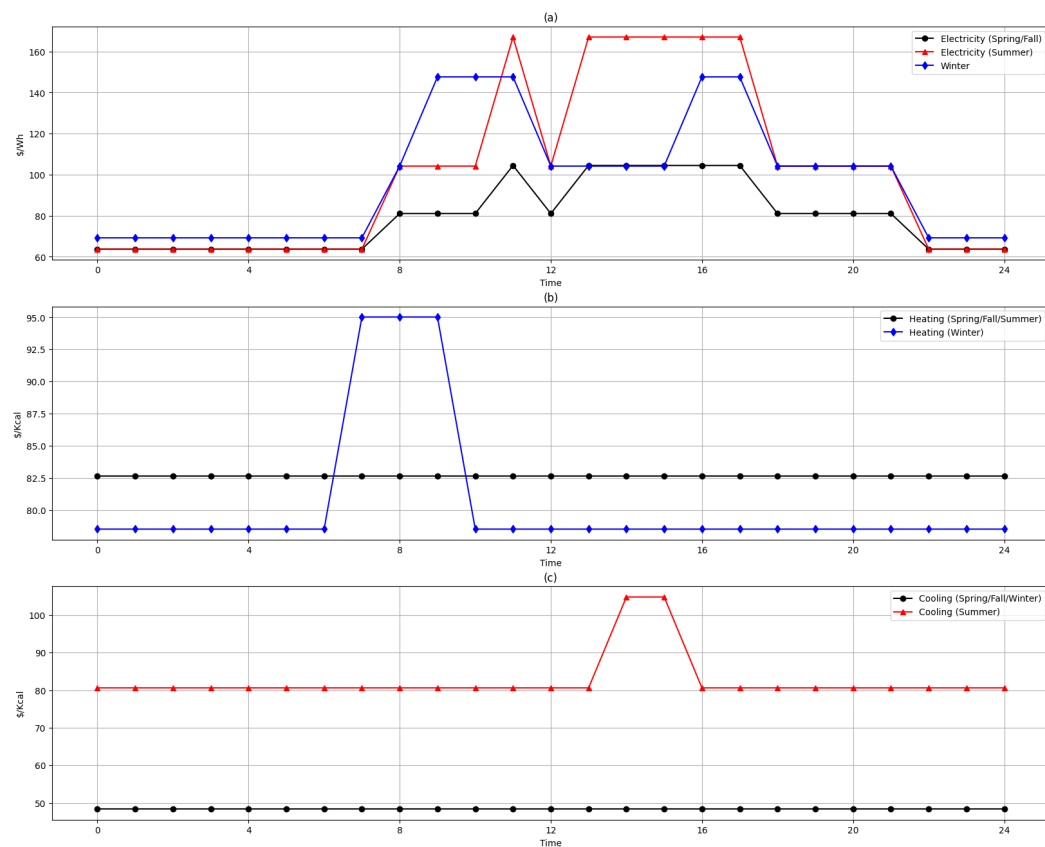


Figure 5. Electricity and thermal energy cost (a) electricity time-of-use tariff (b) heating pricing tariff (c) cooling pricing tariff.

6.3. Modeling CHP

A combined heat and power (CHP) system is an integrated energy system that uses the same fuel to generate two different types of energy (heat and electricity) simultaneously, typically using the hot part for electricity and the cold part for heat. In particular, since factories use both electricity and heat as energy sources, it can significantly reduce energy costs when applied to industrial complexes. By utilizing CHP in factories, thermal energy can be used to recover hot water from cooling water and exhaust gas generated during the process, thus producing as much energy as possible with the same amount of fuel.

The operating curve of a CHP system is critical to understanding the performance characteristics of a CHP system, planning operations, and optimizing efficiency. By analyzing the operating curve, system operators can determine the optimal conditions to achieve the desired balance between electricity and heat production while maximizing the energy efficiency and cost-effectiveness of the systems. As presented in Figure 6, the operating curve of a CHP system can be represented by a graph with heat output on the X-axis and power output on the Y-axis. The operating curve typically has a linear or non-linear shape and can be different depending on the system's characteristics. In general, CHP systems aim to produce power and heat simultaneously. On the operating curve, at a certain power output, the system provides maximum heat output, and vice versa, at a certain heat output, the system provides maximum power output. In Spot D, the operator produces maximum electricity while consuming maximum fuel, while in Spot C, both heat and electricity can be produced at a high rate. Spot B can operate with maximum fuel savings, while Spots A and D produce only electricity. Therefore, the CHP system selects the optimal operating point for different load conditions to achieve maximum efficiency and energy utilization.

The operating curve provides important information for the design and performance of a CHP. By analyzing a system's operating curve, the operator can identify the optimal operating conditions for specific power and heat requirements. This allows the operator to maximize energy efficiency and optimize the performance of the system. Assume the CHP is extraction-condensing steam turbines, which has more flexible thermoelectric operation characteristics and is commonly used in integrated energy systems such as microgrid and FEMS. The curve pattern under typical operating conditions for a CHP is shown in Figure 6. As the heat output changes, the applicable upper and lower limits also change. The point of operation for all these possible regions can be described by a set of convex corner points, as shown in (3)–(5).

$$H_t^{CHP} = \sum_{k=1}^{CP} (\alpha_t^k \cdot H^k) \quad (3)$$

$$P_t^{CHP} = \sum_{k=1}^{CP} (\alpha_t^k \cdot P^k) \quad (4)$$

$$\sum_{k=1}^{CP} \alpha_t^k = 1, 0 \leq \alpha_t^k \leq 1 \quad (5)$$

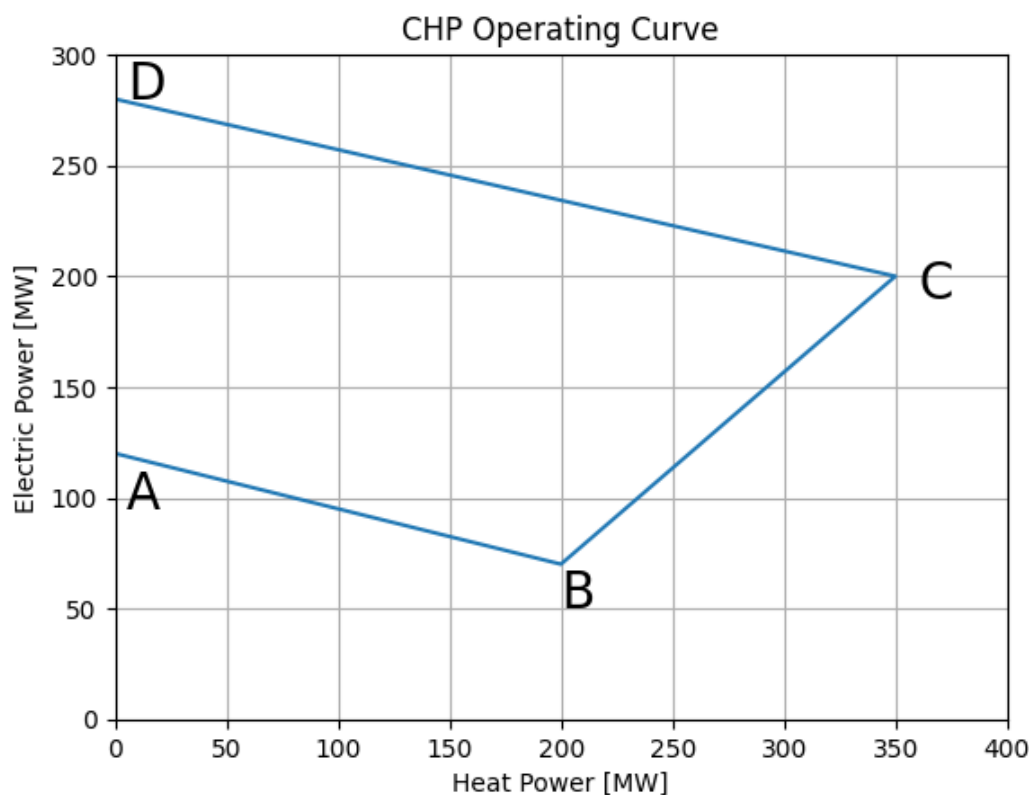


Figure 6. Feasible operating condition curve of CHP.

The operating cost of a CHP can be represented as follows:

$$C_t^{CHP} = \sum_{k=1}^{CP} (\alpha_t^k \cdot C^k) \quad (6)$$

where H_t^{CHP} represents the heat output at the point of operation of the CHP at the current time t , CP is the number of corner points in the CHP's operable condition curve, α_t^k is the coefficient of combination of the k -th corner point in the operating curve of CHP at time t . H^k represents heat output corresponding to the k -th corner point in the feasible operating

curve of the CHP. P_t^{CHP} represents the power output of the current operating point at time t , P^k represents power output that corresponds to the k -th corner point in the realizable operating curve of the CHP [23].

6.4. Modeling VRFB

To estimate the capacity and performance required to deploy a VRFB, the following modeling can be inferred. The cell voltage of VRFB can be defined as the electromotive force at 50% SOC, represented as follows:

$$V_{cell} = V_{OCV} + IR_{cell} + \eta_{act} + \eta_{con} \quad (7)$$

$$V_{OCV} = V_0 + \frac{RT}{zF} \ln\left(\frac{C_{V^{5+}}(C_{H^+})^2 C_{V^{2+}}}{C_{V^{4+}} C_{V^{3+}}}\right) \quad (8)$$

where I is cell current and R_{cell} is the resistance of the cell.

The state of charge (SOC) is the proportion of the concentration of vanadium-ions in the electrolyte, which can be represented as:

$$SOC = \frac{Q_{Charge}}{Q_t} = \frac{C_{V^{2+}}}{C_{V^{2+}} + C_{V^{3+}}} + \frac{C_{V^{5+}}}{C_{V^{4+}} + C_{V^{5+}}} \quad (9)$$

Ideal capacity stored in a given volume of VRFB's electrolyte can be represented as follows:

$$Q_t = \frac{I}{n \times F \times C \times SOC_{min}} \quad (10)$$

System efficiency (SE) is the proportion of VRFB's discharge output to charge power, and open circuit voltage is the cell voltage in the complete absence of external current, which can be defined as follows:

$$SE = \frac{\int_0^{t_{dis}} (P_{dis} - P_{loss}) dt}{\int_0^{t_{ch}} (P_{ch} + P_{loss}) dt} \times 100 \quad [\%] \quad (11)$$

where t_{dis} and t_{ch} are the charging time and discharging time, respectively. P_{dis} and P_{ch} are the power output of the discharging and charging, respectively. P_{dis} is power loss, which can occur in both charging and discharging [24,25]. Since VRFBs are built for long-term operation, it is economically beneficial to prioritize ways to minimize energy losses from charging and discharging. Therefore, it can be beneficial to deploy all VRFBs even if the initial deployment cost is high.

6.5. The Main Load of Bio-Manufacturing Factory

A major energy-consuming load in bio-manufacturing is the cooling/chilled water system. A simplified representation of the main loads used in the bio-manufacturing process is shown in Figure 7. These loads have a high consumption of both electricity and thermal energy, so high levels of energy savings can be expected by utilizing ESS and CHP. The cooling water system in a biotechnology factory operates to provide cooling and refrigeration for various processes. It functions as follows and receives the input of cold water.

- Chiller: in a biotechnology factory, maintaining a consistent temperature is crucial for numerous processes and equipment. The chiller generates cold water to cool down these processes and equipment. The chiller typically utilizes a compressor and refrigerant to produce cold water, where the refrigerant absorbs and releases heat through compression and expansion, resulting in a cooling effect.
- Cooling Tower: the cooling tower is employed to supply cooled water. The cold water produced by the chiller is directed to the cooling tower, where heat exchange takes place. The cooling tower operates by releasing heat to the atmosphere, thereby

reducing the temperature of the cold water. The cooled water is then recirculated back to the chiller for reuse.

- Water Tank: the water tank plays a vital role in a cooling system, ensuring a reliable supply of chilled water and availability of water when needed. The water tank is responsible for storing the chilled water produced by the cooling system. Cold water supplied from the chiller or cooling tower is pumped into the water tank for storage. The pump efficiently moves the stored chilled water and supplies it to the designated locations. The water tank is designed to have a sufficient capacity to store an adequate amount of chilled water.

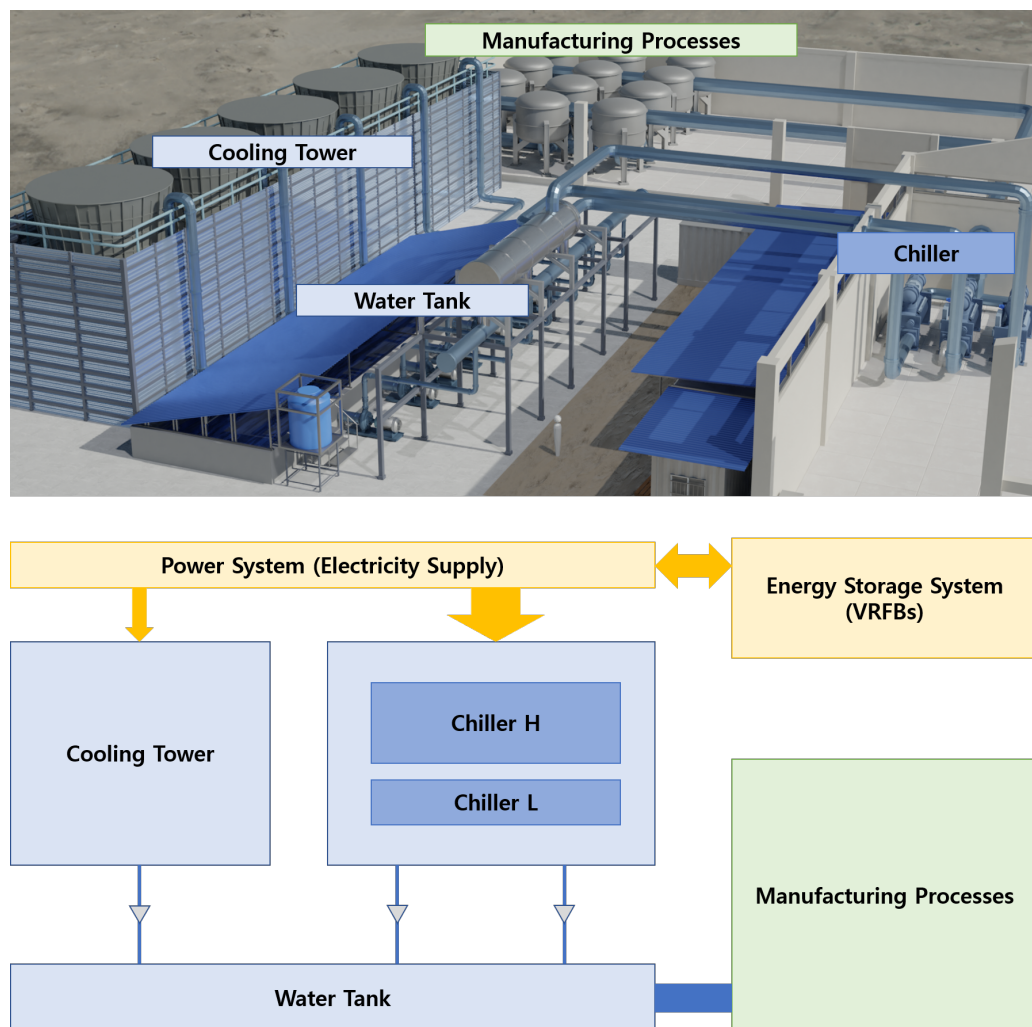


Figure 7. Digital twin models and energy system schematics of bio-manufacturing factory.

The temperature of the chilled water required in a bio-industrial plant will vary depending on the product being produced and the season. Therefore, FEMS in bio-processing must monitor temperature, flow, pressure, etc., at each control point to ensure that chilled water is delivered at the temperature required by the manufacturing process. At this time, cooling towers and chillers are used to maintain the temperature of the water bath, which consumes a lot of energy, so CHP and ESS can be used to reduce energy. Through CHP's recovery and supply of thermal energy and ESS's charge/discharge scheduling, unnecessary operation of cooling towers and chillers can be reduced. Figure 8 shows the pattern of the main loads and temperature in bio-manufacturing factory. Each load is characterized by its season, driving conditions, and product production.

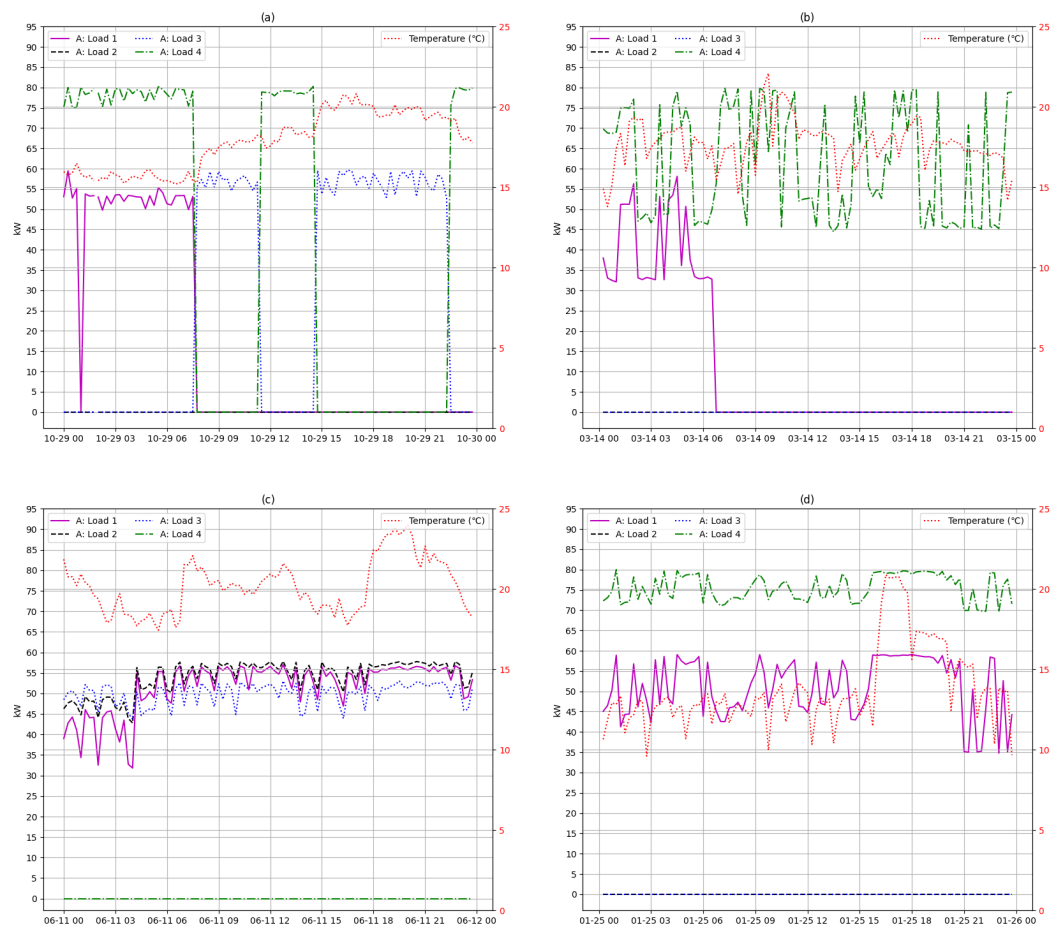


Figure 8. Patterns of main loads and temperature variations in the bio-manufacturing. (a) Load and temperature patterns in the fall; (b) load and temperature patterns in the spring; (c) load and temperature patterns in the summer; (d) load and temperature patterns in the winter.

A:Load 1 operates primarily from 00:00 to 08:00 during the spring and fall seasons. Except for the early morning hours in spring, when A:Load 1 is turned off, A:Load 3 is operated, but A:Load 1 and A:Load 3 are not operated at the same time because they are equipped to meet different temperature conditions. In addition, A:Load 2 is mainly operated during the summer months when the temperature is high, as shown in Figure 8b. A:Load 4 is only operated during certain hours of the day, as shown in Figure 8a, and is not operated during the summer months. Each load is operated to achieve a specific temperature condition, and this specific condition is affected by the season but can also vary depending on the items being produced in the factory, which is why the FEMS needs to be linked to the MES system.

6.6. The Main Load of Paper-Manufacturing Factory

The paper industry, similarly to the bio industry, has many loads that require both thermal and electrical energy, so ESS and CHP can be used to achieve high energy savings. In particular, drying and heating systems are loads that require constant high energy consumption during the manufacturing process. A simplified representation of the main loads used in the paper manufacturing process is shown in Figure 9: compressor, dryer, milling machines, heating, etc. To produce paper and pulp, raw materials are first broken down and mixed into a slurry, then milled and shaped into paper using a milling machine, then dried and heated, and finally processed into paper using compressed air. Paper production is one of the most energy- and resource-intensive industries, so sustainable production methods, such as improving the efficiency of the production process and actively using recycling, are important from an environmental perspective.

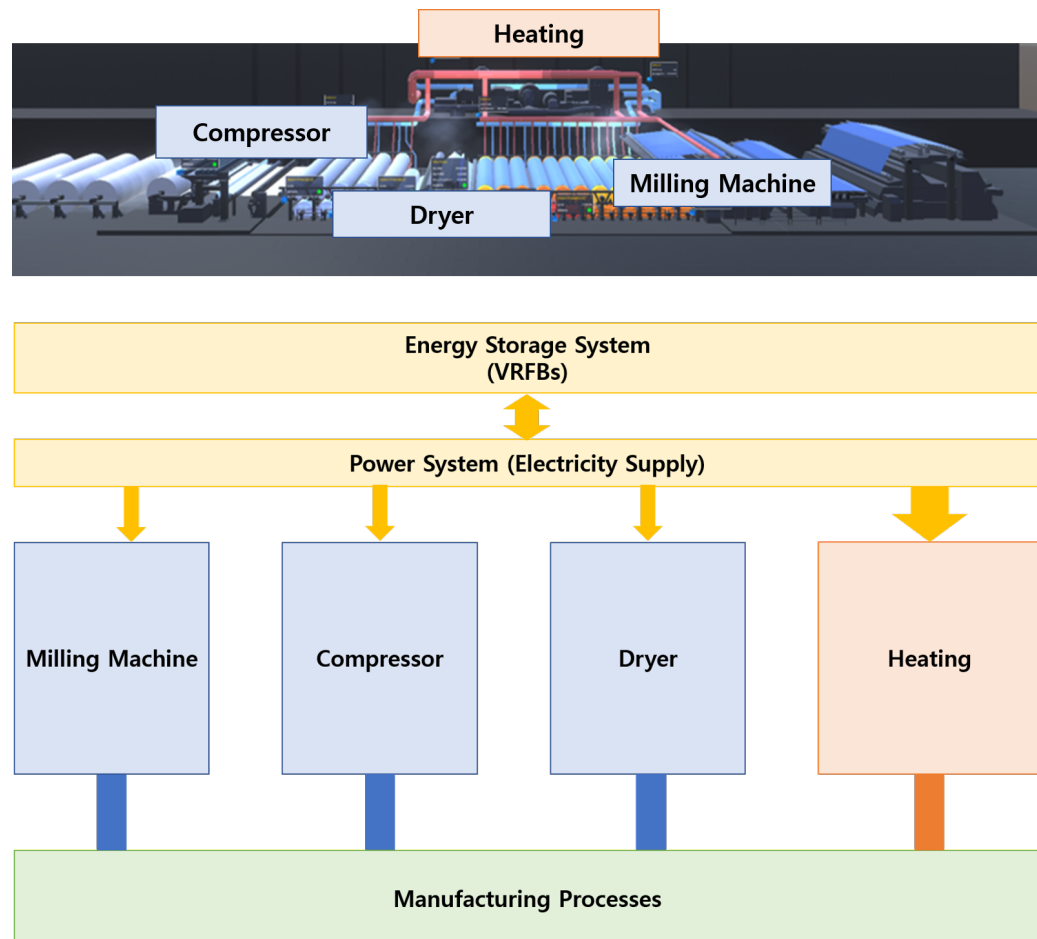


Figure 9. Digital twin models and energy system schematics of paper-manufacturing factory.

Load

- **Milling Machine:** milling machines are important pieces of equipment in the paper/pulp making industry, contributing to the production of quality paper through the grinding and processing of materials. A milling machine is responsible for crushing wood pulp into fibers. It finely grinds the wood material to separate the fibers individually. These crushed wood fibers are then used as the material needed to make paper.
- **Compressor:** compressed air is used to power the machines used in the papermaking process, and it is also used to remove the impurities generated during the papermaking process. Compressed air can also be used to monitor the condition of the pulp and to maintain the equipment used in the paper process.
- **Dryer:** a dryer is responsible for drying paper sheets by maintaining the proper humidity and dryness. This ensures the quality and characteristics of paper products and maintains the stability of the production process. The dryer uses high temperatures and air circulation to remove moisture from the paper sheet and dry it. This ensures that the paper sheet has stable properties and can proceed to the next process step.
- **Heating:** the papermaking process requires water heating. After grinding wood pulp into fibers, water heating is performed to disperse the fibers. During this process, a water heater is used to heat the water. Water heating helps the wood powder and fibers mix properly and improves the properties of the fibers. In the papermaking process, heating is also required during the rolling of paper sheets. Rolling is a process performed to improve the density and surface properties of paper sheets. In the rolling process, heat is used to heat the paper sheet, and pressure is applied through a rolling mill to control the density of the paper sheet. Heating in the dryer helps dry the paper

sheets, as described previously. Inside the dryer is a heating unit, which generates heat to remove moisture from the paper sheets and dry them.

As shown in Figure 10, energy consumption patterns in paper manufacturing and the loads used vary greatly by season. Load 1 is related to heating and consumes more energy than the other loads. Energy consumption in the heating process can vary depending on the heating method, efficiency of the equipment, operating conditions, etc. For efficient energy management, the operator can take measures such as optimizing the operating conditions of the heating system, introducing heat recovery systems to recycle heat, etc. It is also important to minimize heat loss by optimizing insulation and heating times. Heating in the paper industry is a key part of the paper manufacturing process, and proper energy management can ensure efficient operation. In the Figure 10, Loads 2, 3, and 4 are metering points that are measuring the energy usage of a system with multiple loads. Load 2 does not operate during the fall and winter months, but is added to the paper manufacturing process in the spring and summer when temperatures are relatively high. Load 3 is characterized by being repeatedly turned on and off as a milling machine-like load, largely independent of the seasons, and Load 4 is operated according to the characteristics of the paper being produced, except in the cold winter months when the temperature is lower.

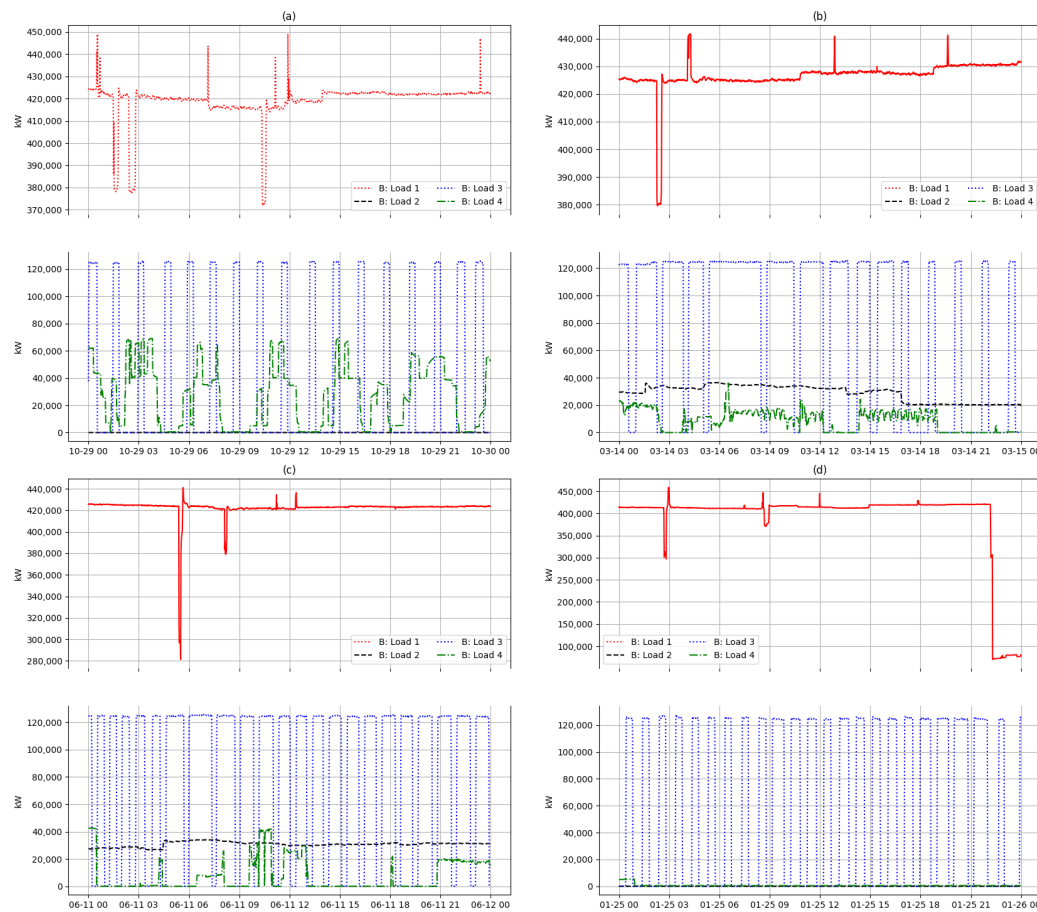


Figure 10. Patterns of main loads and temperature variations in the paper-manufacturing. (a) Load and temperature patterns in the fall; (b) load and temperature patterns in the spring; (c) load and temperature patterns in the summer; (d) load and temperature patterns in the winter.

7. LCOE for the Hybrid System

7.1. Capital Cost and LCOE

The LCOE approaches for PV are well documented in [26–28]. The LCOE of CHP is a little more complicated due to the potentially unknown expenditure on carbon dioxide

emissions, in addition to considering the power produced, investment costs, discount rate, fuel costs, operation and maintenance costs, carbon costs, decommissioning costs, etc. [29–31]. The LCOE needs to determine the cost of energy production according to modeling and energy dataset; it provides the cost of energy in units of (\$/kWh) for the hybrid system. Since LCOE is highly sensitive to input, a sensitivity analysis is performed based on the input assumptions. To calculate the LCOE of VRFB, CHP and PV with the given specifications, there are a few factors and assumptions involved [18,32].

- Capital cost of the hybrid systems:
 1. PV: \$500/kW–\$4000/kW
 2. VRFB: \$350/kW–\$500/kW
 3. CHP: \$500/kW–\$1400/kW
- The maximum efficiency of the PV inverter is 93–95%, the efficiency of CHP is 80–98%, the efficiency of the VRFB is 80–90%
- The interest rate is 0–10% and discount rate 0–10%
- Fuel cost of natural gas used in the CHP is \$6–15/MMBTU

Initial installation costs include PV, VRFB, and CHP modules and they are calculated as follows:

$$I = I_{pv} + I_{chp} + I_{VRFB} \quad (12)$$

Operations and maintenance (O&M) costs includes the O&M of the PV including inverter replacement (O_{pv} , M_{pv}), CHP modules and variable operations and maintenance costs associated with the CHP modules. CHP module costs (O_{chp} , M_{pv}) and VRFB replacement costs (R_{VRFB}):

$$O = O_{pv} + O_{chp} + M_{pv} + M_{chp} + R_{VRFB} \quad (13)$$

VRFBs have very little replacement cost (R_{VRFB}) compared to lithium-ion batteries. The LCOE of the hybrid energy system can be represented as follows:

$$LCOE = \frac{I + \sum_{n=1}^T \frac{(I \times i + O + F_{chp})}{(1+d_r)^n}}{\sum_{n=1}^T E_{PV} \times (1 - d_{PV})^n + \frac{E_{chp} \times (1 - d_{CHP})^n}{(1+d_r)^n}} \quad (14)$$

where E_{pv} is rated energy from PV per year (kWh/year), C_{PV} is the capacity of PV system, CF_{PV} is capacity factor of PV system, d_{pv} is performance degradation rate of the PV yearly, d_{chp} is degradation rate of the CHP yearly, which can be calculated as follows:

$$E_{pv} = 24 \text{ h} \times 365 \text{ /year} \times C_{PV} \times CF_{PV} \quad (15)$$

and E_{chp} is rated energy from CHP per year (kWh/year), C_{CHP} is the capacity of CHP system, CF_{CHP} is capacity factor of CHP system, which can be calculated as follows:

$$E_{chp} = 24 \text{ h} \times 365 \text{ /year} \times C_{CHP} \times CF_{CHP} \quad (16)$$

and the fuel cost can be determined by dividing the sum of the total heat and electricity produced by the CHP by the efficiency of the CHP unit. The fuel cost of CHP (F_{CHP}) can be calculated as follows:

$$F_{chp} = F_{fuel} \times F_c \times h_{chp} \quad (17)$$

$$F_{fuel} = \frac{(E_{chp} \times 3.143) + T_{chp}}{Eff_{chp}} \quad (18)$$

where F_{fuel} is fuel consumed by the CHP unit per year (MMBTU/year), F_c is the cost of fuel per unit thermal energy (\$/MMBTU) and h_{chp} is the operating time in a year (h). E_{CHP} is

electrical power output of the CHP (kW), T_{CHP} is the thermal output of CHP (MMBTU/h) and Eff_{CHP} is the efficiency of the CHP.

7.1.1. System Cost and Financing

The cost, financing terms and efficiency of PV, VRFB and CHP can vary depending on the energy capacity and power output of products, the life time of the project on investor, country and location. In addition, capital/install costs are gradually decreasing as renewable energy penetration increases. The reference values such as interest rates, discount rates for LCOE used in this study are taken from the IEA's Projected Costs of Generating Electricity 2020 [33].

Therefore, the LCOE of a hybrid energy system is sensitive to the cost of the system. Due to advances in technology, PV are available at historically low prices, such as \$0.4/W in [34]. For the case study, the capital cost of PV is assumed to be \$500/kW, the capital cost of VRFB is assumed to be \$400/kW and the installation cost of CHP is assumed to be \$900/kW.

7.1.2. Life Time and Degradation Rate

The life expectancy of the hybrid energy system depends on the lifetime expectancy of the PV and CHP. It is assumed that the VRFB has a relatively long cycle of more than 20 years and can be operated with long-term maintenance, including replacement costs and electrolyte replenishment. The average PV is conservatively assumed to have a lifespan of 25 years, but can be operated for a longer period of time if efficiency decline is taken into account. The life expectancy of CHP is thought to be between 10 and 20 years. Operation and maintenance costs are assumed to increase gradually over time to account for replacement costs of inverters and VRFBs. Fuel costs are referenced to [35] and assumed to decrease slightly each year as reported in [35]. The output of PV is affected by the degradation rate of the PV modules. The degradation rate of PV is about 0.5–1.0%/h [36,37]. This degradation is caused by chemical processes such as oxidation, corrosion, and thermal stress.

The degradation rate of CHP can be affected by the technology type of the prime mover, but the annual degradation rate is less than 0.5% for all technologies [30].

8. Results

As a case study, we analyze the LCOE of installing a hybrid energy system in each of the bio and paper manufacturing factories, and compare the LCOE when the two factories share a hybrid energy system. Because the power and thermal energy consumed by factories can vary by dozens to hundreds of orders of magnitude from that of typical homes and buildings, the hybrid energy systems deployed are primarily aimed at reducing peak loads. In addition, shared ESS can be considered to quickly recover deployment costs.

The installation costs of PV are above the average and are assumed to be \$400/kW and the minimum capital cost of the PC is \$500/kW. The capacity of PV required to meet demand is 900 kW. CHP, on the other hand, assumes a capital cost of \$900/kW with an engineering cost of \$450 [30]. CHP units have a minimum cost range of \$800–1400/W [32]; therefore, a minimum capital cost of \$500/kW is considered. In this case study, the VRFB-ESS has an installed capacity of 10 MWh (2 MW for 5 h). As we saw above, bio-manufacturing processes consume a lot of power and thermal energy in their cooling systems, with an average electric demand of 90,000 MWh/year and thermal demand of 500 MMBTU/year. The paper industry is one of the most energy-consuming industries in the world, and this paper-factory is large enough to account for 30% of South Korea's paper production, with an average electric demand of 200,000 MWh/year and thermal demand of 2000 MMBTU/year. Considering the geographical environment and structure of the factories, 1 MW of PV is assumed to be installed at the bio-manufacturing factory and 3 MW at the paper-manufacturing factory. The manufacturing in bio and paper produces biogas as a byproduct of wastewater

treatment, which can be used as a feedstock to run a CHP; assume a 2 MWe CHP that can utilize natural gas and biogas.

As shown in Figure 11, the LCOE of a hybrid energy system is highly dependent on the financing scenario. The LCOE of the hybrid system with different discount rates of 3%, 5%, 7%, and 9% are shown, with interest rates = 1% with all other conditions maintained for a loan term varying from 25 years. The LCOE for the hybrid system when the discount rate is 9% is \$0.275; when the discount rate is 7% is 0.235; when the discount rate is 5% is \$0.224/kWh at 25 years; when discount rate is 3% is 0.212/kWh at 25 years.

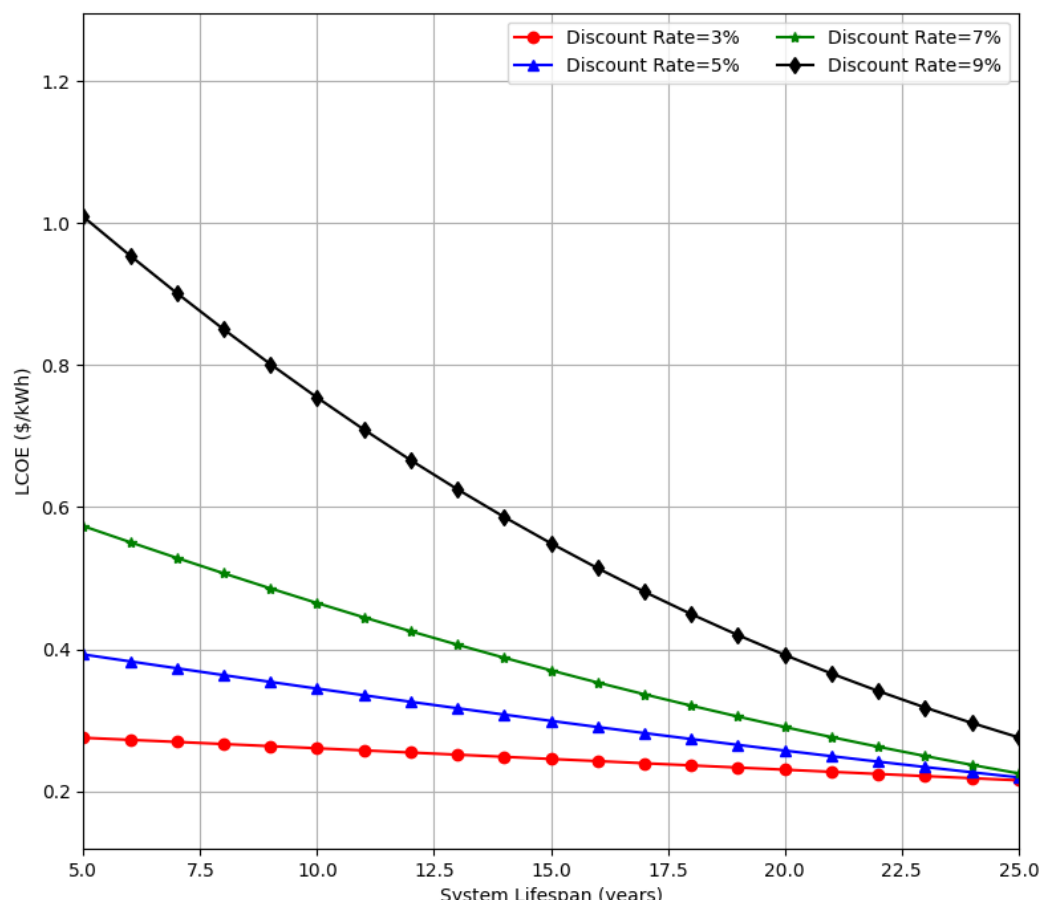


Figure 11. LCOE of the hybrid energy system for different discount rate (interest rates = 1%).

9. Limitations and Future Work

A methodology for roughly estimating the LCOE of PV, VRFB-ESS, and CHP systems has been presented. This methodology was conducted at the simulation level to determine the LCOE of a hybrid energy system that could be installed in an industrial facility in South Korea. We calculated an estimate of the capacity needed based on actual load data. LCOE can vary depending on each country's energy policies, financing terms, installation costs, industrial electricity/heat tariffs, etc. In addition, since not all loads in the factory are currently being monitored, accurate estimates of power and thermal energy usage are not available, and a real-time metering and monitoring system must be implemented to estimate them. VRFBs are an economically favorable ESS in the long run, but they require a large footprint, so real estate costs may need to be considered in addition. Estimating the return on investment and payback period depends on the amount of energy savings each plant is targeting by utilizing ESS, PV, and CHP, as well as how the energy storage system is operated. However, if an optimized hybrid energy system is operated, the initial investment cost can be recovered quickly by using incentives according to each country's policy. Therefore, future studies should consider more load data and operating conditions.

Based on various operating conditions and scenarios, the return on investment and payback cost will be estimated, and the optimized operation plan will be tested.

10. Conclusions

VRFBs have a favorable LCOE when considering all the costs of operating an ESS, including initial facility investment, maintenance, and charging/discharging costs, due to their long lifetime and low annual energy/capacity decline rate. The high annual energy/capacity decline rate of lithium-ion-based energy storage devices is also a major disadvantage in terms of maintenance costs, as they require augmentation to add new batteries during operation, whereas VRFBs do not. In addition, the electrolyte, which accounts for 40–60% of the total battery cost, has a very small reduction rate, so the residual value of the electrolyte is high after operation is completed, and the electrolyte can be recycled, making it an eco-friendly battery. Of course, VRFBs also have disadvantages, such as their large volume, which requires a large site to be utilized as an energy storage device, and their low energy efficiency compared to lithium-ion batteries, which requires a high initial construction cost for the same energy/capacity. In order to solve the volume problem of VRFBs, research and improvements regarding the structure are being continuously conducted. In addition, in industrial complexes and power generation complexes, energy efficiency is important, but stability is more important, so the introduction of VRFBs is viewed positively, and it is expected that energy efficiency and initial investment costs can be recovered through long-term ESS operation.

Author Contributions: S.H.K. developed the main idea and designed the proposed model; S.H.K. conducted the simulation studies and wrote the paper. Y.D. and T.-W.H. contributed to the editing of the paper. Y.D., I.W.L. and T.-W.H. are responsible for acquiring and providing the actual factory data. All authors have read and agreed to the published version of the manuscript.

Funding: This research was funded by Korea Institute of Energy Technology Evaluation and Planning (No. KETEP-20202020800290 & 20202020900290).

Data Availability Statement: The data presented in this study are available upon request from the corresponding author. The data are not publicly available due to corporate confidentiality requirements.

Conflicts of Interest: The authors declare no conflict of interest.

Abbreviations

The following abbreviations are used in this manuscript:

AI	Artificial Intelligence
CHP	Combined Heat and Power
CCHP	Combined Cooling, Heat and Power
FEMS	Factory Energy Management System
EIA	The U.S. Energy Information Administration
DER	Distributed Energy Resources
ESS	Energy Storage System
IEA	International Energy Agency
LCOE	Levelized Cost of electricity
RFB	Redox Flow Batteries
ROI	Return of Investment
PV	Photovoltaics
VRFB	Vanadium Redox Flow Battery

References

- Wei, Y.M.; Chen, K.; Kang, J.N.; Chen, W.; Wang, X.Y.; Zhang, X. Policy and Management of Carbon Peaking and Carbon Neutrality: A Literature Review. *Engineering* **2022**, *14*, 52–63. [[CrossRef](#)]
- IEA. An Energy Sector Roadmap to Carbon Neutrality in CHINA. 2021. Available online: <https://www.iea.org/reports/an-energy-sector-roadmap-to-carbon-neutrality-in-china> (accessed on 27 June 2023).

3. Zhao, X.; Ma, X.; Chen, B.; Shang, Y.; Song, M. Challenges toward carbon neutrality in China: Strategies and countermeasures. *Resour. Conserv. Recycl.* **2022**, *176*, 105959. [[CrossRef](#)]
4. Lee, S.; Nengroo, S.H.; Jin, H.; Doh, Y.; Lee, C.; Heo, T.; Har, D. Anomaly detection of smart metering system for power management with battery storage system/electric vehicle. *ETRI J.* **2022**, *1*–16. [[CrossRef](#)]
5. Hanshin, Y.; Kim, J.H. Vanadium Redox Flow Battery Development and Domestic Demonstration. *J. Electr. World Mon. Mag.* **2014**, *6*, 48–54.
6. Mongird, K.; Viswanathan, V.; Alam, J.; Vartanian, C.; Sprenkle, V.; Baxter, R. 2020 grid energy storage technology cost and performance assessment. *Energy* **2020**, *2020*, 6–15.
7. Tian, Y.; An, Y.; Zhang, B. Approaching Microsized Alloy Anodes via Solid Electrolyte Interphase Design for Advanced Rechargeable Batteries. *Adv. Energy Mater.* **2023**, *13*, 2300123. [[CrossRef](#)]
8. Weber, A.Z.; Mench, M.M.; Meyers, J.P.; Ross, P.N.; Gostick, J.T.; Liu, Q. Redox flow batteries: A review. *J. Appl. Electrochem.* **2011**, *41*, 1137–1164. [[CrossRef](#)]
9. Wang, W.; Luo, Q.; Li, B.; Wei, X.; Li, L.; Yang, Z. Recent progress in redox flow battery research and development. *Adv. Funct. Mater.* **2013**, *23*, 970–986. [[CrossRef](#)]
10. Khaki, B.; Das, P. Definition of multi-objective operation optimization of vanadium redox flow and lithium-ion batteries considering leveled cost of energy, fast charging, and energy efficiency based on current density. *J. Energy Storage* **2023**, *64*, 107246. [[CrossRef](#)]
11. Aramendia, I.; Fernandez-Gamiz, U.; Martinez-San-Vicente, A.; Zulueta, E.; Lopez-Gude, J.M. Vanadium redox flow batteries: A review oriented to fluid-dynamic optimization. *Energies* **2020**, *14*, 176. [[CrossRef](#)]
12. Khawaja, Y.; Giaouris, D.; Patsios, H.; Dahidah, M. Optimal cost-based model for sizing grid-connected PV and battery energy system. In Proceedings of the 2017 IEEE Jordan Conference on Applied Electrical Engineering and Computing Technologies (AEECT), Aqaba, Jordan, 11–13 October 2017; pp. 1–6. [[CrossRef](#)]
13. Guo, F.; Wu, X.; Liu, L.; Ye, J.; Wang, T.; Fu, L.; Wu, Y. Prediction of remaining useful life and state of health of lithium batteries based on time series feature and Savitzky-Golay filter combined with gated recurrent unit neural network. *Energy* **2023**, *270*, 126880. [[CrossRef](#)]
14. Deng, Q.; Lin, B. Automated machine learning structure-composition-property relationships of perovskite materials for energy conversion and storage. *Energy Mater.* **2021**, *1*, 100006. [[CrossRef](#)]
15. Liang, J.; Wu, T.; Wang, Z.; Yu, Y.; Hu, L.; Li, H.; Zhang, X.; Zhu, X.; Zhao, Y. Accelerating perovskite materials discovery and correlated energy applications through artificial intelligence. *Energy Mater.* **2022**, *2*, 200016. [[CrossRef](#)]
16. Yan, R.; Wang, Q. Redox-Targeting-Based Flow Batteries for Large-Scale Energy Storage. *Adv. Mater.* **2018**, *30*, 1802406. [[CrossRef](#)]
17. Dai, Y.; Chen, L.; Min, Y.; Chen, Q.; Hu, K.; Hao, J.; Zhang, Y.; Xu, F. Dispatch Model of Combined Heat and Power Plant Considering Heat Transfer Process. *IEEE Trans. Sustain. Energy* **2017**, *8*, 1225–1236. [[CrossRef](#)]
18. Lai, C.S.; McCulloch, M.D. Levelized cost of electricity for solar photovoltaic and electrical energy storage. *Appl. Energy* **2017**, *190*, 191–203. [[CrossRef](#)]
19. IEA. Grid-Scale Storage. 2023. Available online: <https://www.iea.org/energy-system/electricity/grid-scale-storage> (accessed on 27 June 2023).
20. EIA. Annual Energy Outlook 2023: Industrial Sector Key Indicators and Consumption. 2023. Available online: <https://www.eia.gov/outlooks/aoe/data/browser/#/?id=6-AEO2023&cases=ref2023&sourcekey=0> (accessed on 22 June 2023).
21. Nelson, D.; Nehrir, M.; Wang, C. Unit sizing of stand-alone hybrid wind/PV/fuel cell power generation systems. In Proceedings of the IEEE Power Engineering Society General Meeting, San Francisco, CA, USA, 16 June 2005; Volume 3, pp. 2116–2122. [[CrossRef](#)]
22. Keyhani, A. *Design of Smart Power Grid Renewable Energy Systems*; John Wiley & Sons: Hoboken, NJ, USA, 2016.
23. Wei, W.; Shi, Y.; Hou, K.; Guo, L.; Wang, L.; Jia, H.; Wu, J.; Tong, C. Coordinated flexibility scheduling for urban integrated heat and power systems by considering the temperature dynamics of heating network. *Energies* **2020**, *13*, 3273. [[CrossRef](#)]
24. Yao, Y.; Lei, J.; Shi, Y.; Ai, F.; Lu, Y.C. Assessment methods and performance metrics for redox flow batteries. *Nat. Energy* **2021**, *6*, 582–588. [[CrossRef](#)]
25. Huang, Z.; Mu, A.; Wu, L.; Wang, H. Vanadium redox flow batteries: Flow field design and flow rate optimization. *J. Energy Storage* **2022**, *45*, 103526. [[CrossRef](#)]
26. Darling, S.B.; You, F.; Veselka, T.; Velosa, A. Assumptions and the leveled cost of energy for photovoltaics. *Energy Environ. Sci.* **2011**, *4*, 3133–3139. [[CrossRef](#)]
27. Son, Y.; Mukherjee, S.; Mallik, R.; Majmunović, B.; Dutta, S.; Johnson, B.; Maksimović, D.; Seo, G.S. Levelized Cost of Energy-Oriented Modular String Inverter Design Optimization for PV Generation System Using Geometric Programming. *IEEE Access* **2022**, *10*, 27561–27578. [[CrossRef](#)]
28. Branker, K.; Pathak, M.; Pearce, J. A review of solar photovoltaic leveled cost of electricity. *Renew. Sustain. Energy Rev.* **2011**, *15*, 4470–4482. [[CrossRef](#)]
29. Larsson, S.; Fantazzini, D.; Davidsson, S.; Kullander, S.; Höök, M. Reviewing electricity production cost assessments. *Renew. Sustain. Energy Rev.* **2014**, *30*, 170–183. [[CrossRef](#)]
30. Nguyen, T.; Spendelow, J.; Margolis, R. *Levelized Costs of Electricity from CHP and PV*; Department of Energy, Program Record (Office of Solar Energy Technologies & Fuel Cell Technologies): Washington, DC, USA, 2014.

31. Chandler, H.; Nguyen, F.; Remme, U. *Projected Costs of Generating Electricity-Edition 2010*; International Energy Agency, Nuclear Energy Agency, Organization for Economic Co-Operation and Development: Paris, France, 2010.
32. Mundada, A.S.; Shah, K.K.; Pearce, J. Levelized cost of electricity for solar photovoltaic, battery and cogen hybrid systems. *Renew. Sustain. Energy Rev.* **2016**, *57*, 692–703. [[CrossRef](#)]
33. IEA. Levelised Cost of Electricity Calculator. 2020. Available online: <https://www.iea.org/data-and-statistics/data-tools/levelised-cost-of-electricity-calculator> (accessed on 27 June 2023).
34. IEA. Solar PV Global Supply Chains. 2022. Available online: <https://www.iea.org/reports/solar-pv-global-supply-chains> (accessed on 27 June 2023).
35. IEA. End-Use Prices Data Explorer. 2022. Available online: <https://www.iea.org/data-and-statistics/data-tools/end-use-prices-data-explorer> (accessed on 27 June 2023).
36. Belluardo, G.; Ingenhoven, P.; Moser, D. *Medium-Term Degradation of Different Photovoltaic Technologies under Outdoor Conditions in Alpine Area*; Solar Photovoltaics, EURAC Research (European Academy of Bozen/Bolzano): Bolzano, Italy, 2013.
37. Jordan, D.; Smith, R.; Osterwald, C.; Gelak, E.; Kurtz, R. Outdoor PV Degredation Comparison. In Proceedings of the 35th IEEE Photovoltaic Specialists Conference (PVSC '10), Honolulu, HI, USA, 20–25 June 2010; Technical report, CP-5200-47704.

Disclaimer/Publisher's Note: The statements, opinions and data contained in all publications are solely those of the individual author(s) and contributor(s) and not of MDPI and/or the editor(s). MDPI and/or the editor(s) disclaim responsibility for any injury to people or property resulting from any ideas, methods, instructions or products referred to in the content.